

Journal : CARCIN

Article Doi : 10.1093/carcin/bgz100

Article Title : Impacts of the MHC class I-like XNC10 and innate-like T cells on tumor tolerance and rejection in the amphibian *Xenopus*

**OXFORD**  
UNIVERSITY PRESS

## INSTRUCTIONS

- 1. Permissions:** Permission to reproduce any third party material in your paper should have been obtained prior to acceptance. If your paper contains figures or text that require permission to reproduce, please confirm that you have obtained all relevant permissions and that the correct permission text has been used as required by the copyright holders. Please contact [jnls.author.support@oup.com](mailto:jnls.author.support@oup.com) if you have any questions regarding permissions.
- 2. Author groups:** Please check that all names have been spelled correctly and appear in the correct order. Please also check that all initials are present. Please check that the author surnames (family name) have been correctly identified by a pink background. If this is incorrect, please identify the full surname of the relevant authors. Occasionally, the distinction between surnames and forenames can be ambiguous, and this is to ensure that the authors' full surnames and forenames are tagged correctly, for accurate indexing online. Please also check all author affiliations.
- 3. Figures:** If applicable figures have been placed as close as possible to their first citation. Please check that they are complete and that the correct figure legend is present. Figures in the proof are low resolution versions that will be replaced with high resolution versions when the journal is printed.
- 4. Colour reproduction:** Please note that if you opt out of paying for colour online and in print, any figures changed to black and white should be checked carefully in your figures legends for any reference to colour. Please check the black and white versions (these may be available at the end of the paper) and contact us if you have any concerns. Please re-word the legend/text to avoid using reference to colour. Alternatively, please let us know if you wish to pay for print colour reproduction or to have both versions in black and white. Please note that there is a £350/\$600 charge for each figure reproduced in colour in print.
- 5. Missing elements:** Please check that the text is complete and that all figures, tables and their legends are included.
- 6. Funding:** Please provide a Funding statement, detailing any funding received. Remember that any funding used while completing this work should be highlighted in a separate Funding section. Please ensure that you use the full official name of the funding body, and if your paper has received funding from any institution, such as NIH, please inform us of the grant number to go into the funding section. We use the institution names to tag NIH-funded articles so they are deposited at PMC. If we already have this information, we will have tagged it and it will appear as coloured text in the funding paragraph. Please check the information is correct. [red text to be used for suppliers who are tagging the funding]
- 7. Conflict of interest:** All authors must make a formal statement indicating any potential conflict of interest that might constitute an embarrassment to any of the authors if it were not to be declared and were to emerge after publication. Such conflicts might include, but are not limited to, shareholding in or receipt of a grant or consultancy fee from a company whose product features in the submitted manuscript or which manufactures a competing product. The following statement has been added to your proof: 'Conflict of Interest: none declared'. If this is incorrect please supply the necessary text to identify the conflict of interest.
- 8. Abbreviations:** some commonly used abbreviations have been automatically expanded for clarity to readers. By using the tracked changes proof for reference, please check the expanded abbreviations have been made correctly and mark up any corrections (if required) here or by email, listing the line and page numbers your correction refers to.

## MAKING CORRECTIONS TO YOUR PROOF

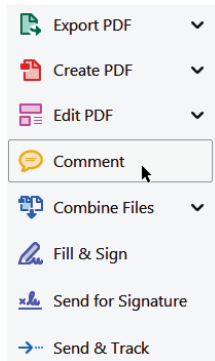
These instructions show you how to mark changes or add notes to your proofs using Adobe Acrobat Professional versions 7 and onwards, or Adobe Reader DC. To check what version you are using go to **Help** then **About**. The latest version of Adobe Reader is available for free from [get.adobe.com/reader](http://get.adobe.com/reader).

### DO NOT OVERWRITE TEXT, USE COMMENTING TOOLS ONLY.

#### DISPLAYING THE TOOLBARS

##### Adobe Reader DC

In Adobe Reader DC, the Comment toolbar can be found by clicking 'Comment' in the menu on the right-hand side of the page (shown below).

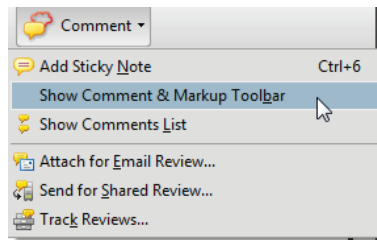


The toolbar shown below will then display along the top.



##### Acrobat Professional 7, 8, and 9

In Adobe Professional, the Comment toolbar can be found by clicking 'Comment(s)' in the top toolbar, and then clicking 'Show Comment & Markup Toolbar' (shown below).

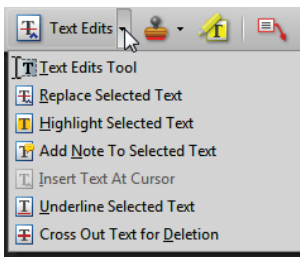


The toolbar shown below will then be displayed along the top.



#### USING TEXT EDITS AND COMMENTS IN ADOBE ACROBAT

This is the quickest, simplest and easiest method both to make corrections, and for your corrections to be transferred and checked.



1. Click **Text Edits**
2. Select the text to be annotated or place your cursor at the insertion point and start typing.
3. Click the **Text Edits** drop down arrow and select the required action.

You can also right click on selected text for a range of commenting options, or add sticky notes.

#### SAVING COMMENTS

In order to save your comments and notes, you need to save the file (**File, Save**) when you close the document.

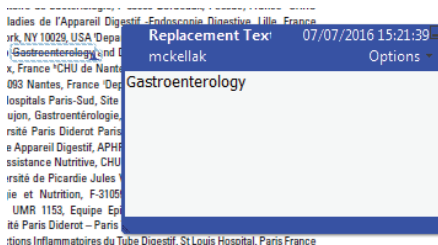
#### USING COMMENTING TOOLS IN ADOBE READER

All commenting tools are displayed in the toolbar. To edit your document, use the highlighter, sticky notes, and the variety of insert/replace text options.

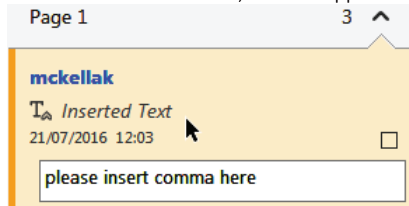


#### POP-UP NOTES

In both Reader and Acrobat, when you insert or edit text a pop-up box will appear. In **Acrobat** it looks like this:



In **Reader** it looks like this, and will appear in the right-hand pane:



## AUTHOR QUERY FORM

Journal : CARCIN

Article Doi : 10.1093/carcin/bgz100

Article Title : Impacts of the MHC class I-like XNC10 and innate-like T cells on tumor tolerance and rejection in the amphibian *Xenopus*

First Author : Maureen Banach






Corr. Author : Jacques Robert

### AUTHOR QUERIES - TO BE ANSWERED BY THE CORRESPONDING AUTHOR

Please ensure that all queries are answered, as otherwise publication will be delayed and we will be unable to complete the next stage of the production process.

Please note that proofs will not be sent back for further editing.

The following queries have arisen during the typesetting of your manuscript. Please click on each query number and respond by indicating the change required within the text of the article. If no change is needed please add a note saying "No change."

<p>AQ1</p> 	<p>Please check that all names have been spelled correctly and appear in the correct order. Please also check that all initials are present. Please check that the author surnames (family name) have been correctly identified by a pink background. If this is incorrect, please identify the full surname of the relevant authors. Occasionally, the distinction between surnames and forenames can be ambiguous, and this is to ensure that the authors' full surnames and forenames are tagged correctly, for accurate indexing online. Please also check all author affiliations.</p>
<p>AQ2</p>  	<p>The term 'neg' in the superscript has been changed to negative (-) symbol (e.g. MHC class II<sup>-</sup>, IgM<sup>-</sup>, etc).</p>
<p>AQ3</p>	<p>Please spell out the acronym 'PLs'.</p>
<p>AQ4</p> 	<p>Figures have been placed as close as possible to their first citation. Please check that they have no missing sections and that the correct figure legend is present.</p>
<p>AQ5</p> 	<p>Please provide the page range for ref. 17.</p>



## ORIGINAL ARTICLE

# Impacts of the MHC class I-like XNC10 and innate-like T cells on tumor tolerance and rejection in the amphibian *Xenopus*

Maureen Banach, Eva-Stina Edholm<sup>1</sup>, Xavier Gonzalez, Abdellatif Benraiss<sup>2</sup> and Jacques Robert<sup>\*,<sup>o</sup></sup>

Department of Microbiology and Immunology, University of Rochester Medical Center, Rochester, NY 14642, USA, <sup>1</sup>The Norwegian College of Fishery Science, UiT The Arctic University of Norway, Tromsø, Norway and <sup>2</sup>Department of Neurology, University of Rochester Medical Center, Rochester, NY 14642, USA

\*To whom correspondence should be addressed. Tel: +1 585 275 1722; Fax: +1 585 473 9573; Email: [jacques\\_robert@urmc.rochester.edu](mailto:jacques_robert@urmc.rochester.edu)

## Abstract

The conditions that lead to antitumor or protumor functions of natural killer T (NKT) cells against mammalian tumors are only partially understood. Therefore, insights into the evolutionary conservation of NKT and their analogs—innate-like T (iT) cells—may reveal factors that contribute to tumor eradication. As such, we investigated the amphibian *Xenopus laevis* iT cells and interacting MHC class I-like (XNC or *mhc1b.L*) genes against ff-2 thymic lymphoid tumors. Upon ff-2 intraperitoneal transplantation into syngeneic tadpoles, two iT cell subsets iVα6 and iVα22, characterized by an invariant T-cell receptor α chain rearrangement (Vα6-Jα1.43 and Vα22-Jα1.32), respectively, were recruited to the peritoneum, concomitant with a decreased level of these transcripts in the spleen and thymus. To address the hypothesis that different iT cell subsets have distinct, possibly opposing, roles upon ff-2 tumor challenge, we determined whether ff-2 tumor growth could be manipulated by impairing Vα6 iT cells or by deleting their restricting element, the XNC gene, XNC10 (*mhc1b10.1.L*), on ff-2 tumors. Accordingly, the *in vivo* depletion of Vα6 iT cells using XNC10-tetramers enhanced tumor growth, indicating Vα6 iT cell-mediated antitumor activities. However, XNC10-deficient transgenic tadpoles that also lack Vα6 iT cells were resistant to ff-2 tumors, uncovering a potential new function of XNC10 besides Vα6 iT cell development. Furthermore, the CRISPR/Cas9-mediated knockout of XNC10 in ff-2 tumors broke the immune tolerance. Together, our findings demonstrate the relevance of XNC10/iT cell axis in controlling *Xenopus* tumor tolerance or rejection.

## Introduction

Sharing characteristics of innate and adaptive immune cells, natural killer T (NKT) cells have recently emerged as relevant immune regulators (1). Akin to innate functions, NKT cells are stimulated via interleukin (IL)-12 and IL-18, without cell expansion, and often independently of T-cell receptor (TCR) engagement (2). Activated NKT cells rapidly produce pro- and anti-inflammatory cytokines, facilitated by the accumulation of pre-made transcripts of interferon gamma (IFN $\gamma$ ) and IL-4 (3). Based on their TCR, NKT cells are categorized into two groups. Type I NKT cells express a TCR composed of Vα14-Jα18 paired to one of three different Vβ in mice, and only one rearrangement

Vα24-Jα18/Vβ11 in humans (4). Due to such limited TCR diversity, type I NKT cells are also known as invariant NKT (iNKT) cells. In contrast, type II NKT cells have a broader TCR repertoire that is still minimally diversified compared to conventional T cells. Expressed on thymocytes, the non-polymorphic major histocompatibility complex (MHC) class I-like CD1d is required for the development of all NKT cells (5). Intriguingly, NKT cells recognize lipids and glycolipids in the context of CD1d with certain glycolipids interacting with either iNKT or type II NKT cells (6). For example, α-galactosylceramide only elicits iNKT cells.

Received: November 28, 2018; Revised: May 27, 2019; Accepted: May 31, 2019

© The Author(s) 2019. Published by Oxford University Press. All rights reserved. For Permissions, please email: [journals.permissions@oup.com](mailto:journals.permissions@oup.com).

## Abbreviations

APBS	amphibian PBS
CTX	<i>Xenopus</i> cortical thymocyte antigen
HDR	homology-directed repair
HLA	human leukocyte antigen
IL	interleukin
iNKT	invariant NKT
ip	intraperitoneal
iTCR	invariant T-cell receptor
KD	knockdown
KO	knockout
MHC	major histocompatibility complex
mAb	monoclonal antibody
NKT	natural killer T
TCR	T-cell receptor
Tg	transgenic
WT	wild-type

NKT cells are crucial regulators of immune responses against pathogens and tumors (7). In tumor immunity, the TCR-based subdivision of NKT cells also reflects their opposing functions. Whereas  $\alpha$ -galactosylceramide-stimulated iNKT cells eradicate tumors, either directly or indirect via CD8 T cells or NK cells, type II NKT cells promote tumor growth via the induction of angiogenesis or recruitment of tumor-associated macrophages (8). Although mouse iNKT cells are antitumoral in diverse cancer models, the stimulation of human iNKT cells in clinical trials have resulted in modest effects on cancers (9). Comparative studies to define how other vertebrates utilize NKT cell analogs—innate-like T (iT) cells in antitumor immune responses—may give insights into conserved functions of these cells. Such knowledge may be valuable in designing better iNKT-based immunotherapies.

The *Xenopus laevis* tadpole is a suitable model to investigate the evolutionary conservation of iT cell functions. An attractive attribute of the tadpole is its suboptimal expression of classical MHC class I molecule compensated by the expression of *Xenopus* MHC class I-like XNC genes (10,11). Similar to mammalian MHC class I-like, XNC genes exhibit low polymorphism and limited tissue distribution. For example, the XNC gene—XNC10 (*mhc1b10.1.L*)—is mainly expressed in the spleen and thymus (12,13). Our previous study using *Xenopus* 15/0 thymic lymphoid tumor cells has revealed that XNC10 expressed on tumor cells promotes *in vivo* tumor growth (14). As XNC10 is restricting a subset of iT cells, defined by the invariant TCR $\alpha$  Va6-Ja1.43 rearrangement (termed Va6 iT cells), it is hypothesized to be a functional analog of CD1d (15). Functionally, Va6 iT cells are required for tadpoles' resistance to infection by the ranavirus Frog Virus 3 as demonstrated by XNC10 reverse genetic loss of function and XNC10 tetramer-mediated depletion (15–17). Recently, we showed that XNC4, restricting Va45 iT cells, was critical in tadpoles' immunity to *Mycobacterium marinum* (18).

Cell sorting followed by deep sequencing in *X.laevis* tadpole spleen has revealed that over 80% of the TCR $\alpha$  repertoire in the CD8-/CD8<sup>low</sup> population is represented by six invariant T-cell receptor (iTCR) rearrangements: the aforementioned Va6-Ja1.43 and Va45-Ja1.14 iTCR along with four others: Va22-Ja1.32, Va23-Ja1.3, Va40-Ja1.22 and Va41-Ja1.40 (15). This suggests the existence of six distinct iT cell subsets (19). In addition to iT cell-mediated immunity to pathogens, we determined whether iT cell subsets participate in immune responses to *Xenopus* ff-2 thymic lymphoid tumor cells, tolerated after transplantation in histocompatible inbred F tadpoles (20). Here, we report that two distinct iT cell subsets are rapidly recruited to the site of ff-2

tumor transplantation. Using loss of function reverse genetics at the organism and tumor levels and XNC10-tetramers, we investigated the roles of XNC10 and Va6 iT in tumor tolerance and rejection.

## Materials and methods

## Tadpoles and ff-2 tumor line

*Xenopus laevis* tadpoles of F inbred strain were obtained from our *Xenopus laevis* Research Resource for Immunology [XLRRRI] (<https://www.urmc.rochester.edu/microbiology-immunology/xenopus-laevis.aspx>). Three week old tadpoles (developmental stage 54–55) were used in all experiments. Animals were anesthetized in 0.1 g/l tricaine methanesulfonate and handled under strict laboratory and UCAR regulations (approval number 100577/2003–151). The ff-2 tumor cell line was derived from a spontaneous thymic lymphoid tumor in an F inbred adult frog in September 1992 (20,21). The cell line has been characterized phenotypically by flow cytometry (CD5<sup>+</sup>, CD8<sup>+</sup>, MHC class I<sup>low</sup>, MHC class II<sup>+</sup>, IgM<sup>+</sup>) and qPCR (expression of C $\mu$ , c-myc, MHC class I<sup>f</sup>, XNC1, 4, 10, 11) as well as by its growth capacity following transplantation into MHC compatible F tadpoles. Tumor clones wild type (WT) and transfectants are stored in aliquots and regularly controlled at the XLRRRI; the last control was performed in July 2018.

Generation of XNC10 KD *X.laevis* embryos and F1 strain on inbred F background

The XNC10 gene was previously deposited in NCBI GenBank: FJ589642.1. Generation of XNC10 KD animals were done via RNAi and I-SceI meganuclease as previously described (15,22). Briefly, I-SceI-hU6-shRNA-XNC10-GFP-I-SceI vector was digested with I-SceI meganuclease for 40 min at 37°C. Eighty picograms of digest was injected into one-cell embryo. Animals were screened for XNC10 deficiency and raised until sexual maturity for intercrossing.

## Generation of XNC10 KO ff-2 tumor cells via the CRISPR/Cas9 system and homology-directed repair

ff-2 cells ( $5 \times 10^6$ ) were nucleofected via Amaxa™-4D-Nucleofection® in 100  $\mu$ l SG solution and CA-137 pulse (Lonza). Two vectors U6-sgRNA-XNC10- $\alpha$ 2-domain-mCherry-Cas9 and XNC10 template with 1000 bp homology arms, flanking EF1 $\alpha$ -tRFP-puromycin cassette, were used equimolarly for a total of 500 ng. Transfected cells were cultured for 24 h before adding puromycin. Transfection efficiency was monitored by flow cytometry. Single cell-derived colonies were obtained by serial dilution.

## Tumor transplantation

Tumor cells ( $1 \times 10^6$ ) in a volume of 10  $\mu$ l of amphibian PBS (APBS) were intraperitoneally transplanted into F tadpoles. For *in vivo* XNC10-T injections, two doses of 1  $\mu$ g XNC10-T in 10  $\mu$ l APBS were intraperitoneally administered per tadpole, 1 day before and 1 day after tumor challenge. Cells were collected by peritoneal lavage.

 $\beta$ 2-m-XNC10-tetramer

XNC10-T consisting of the *X.laevis*  $\beta$ 2-m, a glycine-rich linker, the three XNC10  $\alpha$  domains, a BirA site, a poly-His, and a V5 epitope was produced in Sf9 cells and purified as previously described (15). Eluted fractions were tested by Coomassie blue staining and western blotting with anti-V5-HRP Ab (ThermoFisher). Protein concentration was determined by the Bradford protein assay (Bio-Rad). Protein aliquots were stored at  $-20^\circ\text{C}$ , thawed and used the same day. Biotinylated  $\beta$ 2-m-XNC10 proteins were folded into tetramers by incubation with fluorochrome-labeled streptavidin at a ratio of 5 to 1 over 4 h at RT. The specificity of each batch was tested on adult splenocytes by flow cytometry.

## Flow cytometry

XRRRI provided *X.laevis* antibodies. Transplanted tumors and PLEs were collected by peritoneal lavage, counted with a hemocytometer. Cells were then stained with a *Xenopus* cortical thymocyte antigen (CTX)-specific

2.60

2.65

2.70

AQ2

2.75

2.80

2.85

2.90

2.95

2.100

2.105

AQ3

2.110



monoclonal antibody (mAb) and a fluorophore-goat-anti-mouse secondary Ab (BD Biosciences), followed by *X.laevis*-specific anti-CD8 or anti-MHC class II biotinylated mAbs and streptavidin-fluorophore (BioLegend). To improve the detection of  $V\alpha 6$  iT and CD8 T cells infiltrating tumors in the peritoneum, ff-2 tumor cells were stained with the PKH26 Cell Tracer (Sigma) before transplantation and gated out. XNC10 KO clones were stained with a rabbit anti-XNC10 polyclonal antibody and fluorophore-goat-anti-rabbit Ab (14). The XNC10-T-fluorophore (5–12.5  $\mu$ g) was incubated with PLs (15). Dead cells were excluded with propidium iodide (BD Pharmingen). Five thousand events per sample, gated on live cells, were collected with an Accuri C6 (BD Biosciences). Data were analyzed with FlowJo (TreeStar). The gating strategy is depicted in Figure 1A. Briefly, tumor and leukocyte populations were gated according to size and granularity (FSC-A/SSC-A) and for single cells (SSC-W/SSC-H), then separated into PKH26+ and PKH26- fraction (top panels). As ff-2 tumor cells were stained with PKH26 dye before intraperitoneal transplantation, tumor cells were within the PKH26+ gate. In contrast, PKH26- gate (non-PKH26) included other cells that infiltrated peritoneal cavity following tumor transplantation. Absence of XNC10-T cross-reaction with ff-2 tumor cells was controlled by gating XNC10-T versus CD8 gated on PKH26 at 3 days post-tumor transplantation (middle panels). XNC10-T staining on gated PKH26- cells is shown for three consecutive days after tumor transplantation (bottom panels).

### Cytospin centrifuge and Giemsa staining

Fifty thousand cells in 150  $\mu$ l APBS, supplemented with 20% bovine serum albumin, were cytocentrifuged (Shandon Southern) at 25–30g, 5 min, at RT, air-dried, stained with Giemsa Stain Solution (Gibco) for 3 min, washed in APBS for 10 min and mounted in Permount (Fisher Scientific).

### In vitro cell proliferation assay

Cells were plated at 500,000 cells per well in triplicates, and their numbers were counted at 24, 48 and 72 h using a hemocytometer and Trepan blue exclusion staining. Percentage of cell death was <5% per well.

### Gene expression analysis

RNA and DNA were extracted with TRIzol™ (Invitrogen). cDNA was synthesized using 500 ng DNase-treated RNA, M-MLV RT and oligo(dT) (Invitrogen). One microliter of cDNA or 50 ng of DNA was used for qPCR and PCR, respectively. PCR reactions were resolved on 1.5% agarose gels with EtBr and DNA ladder (Invitrogen). PerfeCTa SYBR® Green FastMix ROX (Quantabio) and ABI 7300 real-time PCR were used for qPCR. For qPCR, the  $\Delta\Delta$ CT method, relative to the endogenous GAPDH and normalized against the lowest expression, was used. All primers were validated by cloning and sequencing amplified products (Supplementary Table 1, available at Carcinogenesis Online).

### Statistical analysis

Statistical analysis was performed with one-way analysis of variance followed by Tukey's *post hoc* test or Student's *t*-test using online software Vassar Stats (<http://vassarstats.net>).

## Results

### Recruitment of $V\alpha 6$ iT cells to the site of tumor transplantation

We previously reported that  $V\alpha 6$  iT cells were detected after 15/0 tumor transplantation in the peritoneal cavity of histocompatible LG-15 tadpoles (14). Here, we investigated whether  $V\alpha 6$  iT cells were also infiltrating the peritoneum after ff-2 tumor intraperitoneal (ip) challenge into inbred MHC homozygous F strain tadpoles. Since mammalian NKT cells are early responders, we determined  $V\alpha 6$  iT cell recruitment within the first 3 days following the tumor challenge. Because ff-2 lymphoid tumor cells express surface CD8, we labeled them with the tracking fluorescent dye PKH26 before transplantation to distinguish tumor cells from infiltrating immune cells (see Materials

and methods). This allowed us to detect an increase of CD8+ T cells at day 3 post-tumor transplantation in a pool of five ff-2 tumor-bearing tadpoles (Figure 1A). In contrast, infiltration of  $V\alpha 6$  iT cells was detected as early as 1 day post-transplantation by using XNC10-tetramer (XNC10-T) and by gating out PKH26+ cells (Figure 1A and B). Notably,  $V\alpha 6$  iT cells were undetectable in the peritoneum of unchallenged tadpoles (16). In addition, we measured the relative abundance of  $V\alpha 6$ - $J\alpha 1.43$  iTCR transcripts. As previously shown,  $V\alpha 6$ - $J\alpha 1.43$  iTCR transcripts were undetectable in the peritoneal cavity of unchallenged or mock-challenged tadpoles (Figure 1C) (16). In agreement with the flow cytometry data,  $V\alpha 6$ - $J\alpha 1.43$  iTCR transcripts increased significantly and gradually after tumor transplantation (Figure 1C). Concomitantly,  $V\alpha 6$ - $J\alpha 1.43$  iTCR significantly decreased in the spleen and thymus and remained unchanged in the liver (Figure 1D–F). Thus, the evidence obtained by two different detection methods suggests that  $V\alpha 6$  iT cells are recruited to the peritoneal cavity from the spleen and thymus following ff-2 tumor transplantation.

### Kinetics of other iT cells after ff-2 tumor challenge

In mammals, iNKT cells are suppressed by protumor type II NKT cells (8). Given that *X.laevis* possesses six iT cell subsets, we were interested to establish whether iT cell subsets other than  $V\alpha 6$  iT cells were recruited to the transplanted ff-2 tumor. Besides  $V\alpha 6$ - $J\alpha 1.43$  iTCR, we monitored the transcript of the other five iTCR $\alpha$  rearrangements upon ff-2 tumor challenge. Four of these iTCR $\alpha$  rearrangements ( $V\alpha 23$ - $J\alpha 1.3$ ,  $V\alpha 45$ - $J\alpha 1.14$ ,  $V\alpha 40$ - $J\alpha 1.22$ ,  $V\alpha 41$ - $J\alpha 1.40$ ) were undetectable in the peritoneum and their expression remained unchanged in the spleen, thymus or liver following tumor transplantation (Supplementary Figure S1, available at Carcinogenesis Online). In contrast, the changes in  $V\alpha 22$ - $J\alpha 1.32$  iTCR transcript levels mirrored the kinetics of  $V\alpha 6$  iTCR, albeit at a lower magnitude (Figure 2). Before or following a mock tumor challenge, the  $V\alpha 22$ - $J\alpha 1.32$  iTCR transcripts were not detected in the peritoneum (Figure 2A). However, the ff-2 transplantation increased  $V\alpha 22$  iTCR in the peritoneal cavity within 1 day post-tumor challenge, in parallel with a decrease of these transcripts in the spleen and thymus, but not in the liver (Figure 2B–D). To examine the  $V\alpha 22$  iTCR relative abundance, we profiled the  $V\alpha 22$  iTCR transcripts in tissues of unchallenged inbred F tadpoles. At comparable levels to  $V\alpha 6$  iTCR,  $V\alpha 22$  iTCR was expressed in the spleen, thymus and intestine, whereas unlike  $V\alpha 6$  iTCR, it was undetected in the lung and expressed at lower levels in the skin (Supplementary Figure S2, available at Carcinogenesis Online). In summary, we identified two different iT cell subsets possibly involved in ff-2 tumor immunity.

### Outcome of ff-2 tumors transplantation into the XNC10 KD F transgenic tadpoles

$V\alpha 6$  iT cells require XNC10 for their development and transgenic (Tg) tadpoles with the XNC10 knockdown (KD) are deficient in  $V\alpha 6$  iT cells (15). To study the fate of transplanted ff-2 tumors in the XNC10 KD tadpoles, we generated inbred F tadpole line with XNC10 KD using RNAi combined with transgenesis (15,22). The specificity of XNC10 gene silencing and the decrease of  $V\alpha 6$ - $J\alpha 1.43$  iTCR expression was confirmed in the spleens of Tg progeny (F1), derived from intercrosses between XNC10 KD Tg inbred F parents (F0) (Supplementary Figure S3, available at Carcinogenesis Online). XNC10 KD Tg F1 tadpoles and age-matched WT controls were then transplanted with ff-2 tumor cells. Using flow cytometry and an mAb that specifically recognizes the CTX, we detected ff-2 tumor cells as previously published

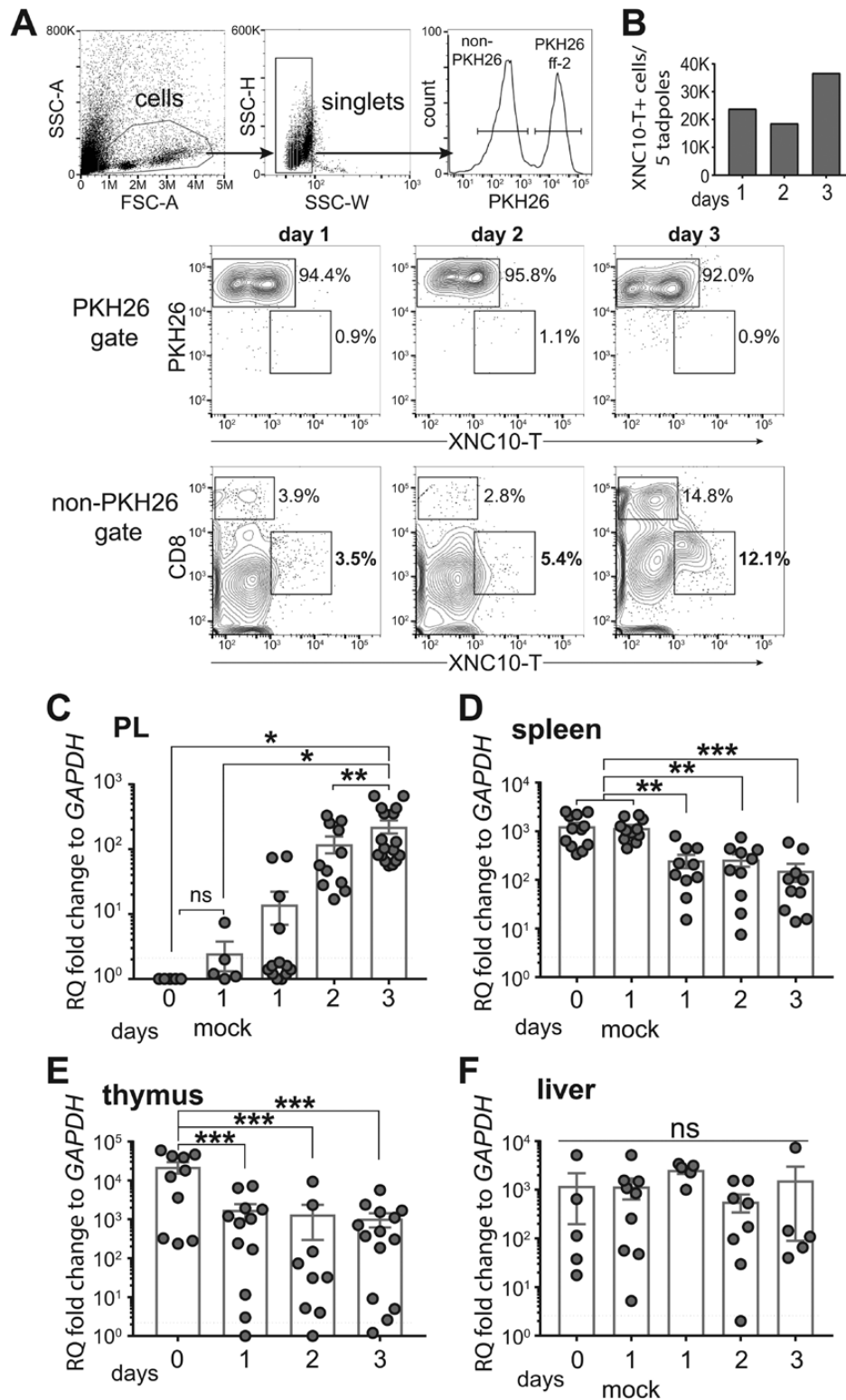


**Figure 1.** Kinetics of Va6 iT cells after ff-2 tumor transplantation. Tadpoles at the developmental stage 54–55 were challenged ip with  $1 \times 10^5$  ff-2 tumor cells. Peritoneal cells, spleen, thymus and liver were collected from un-, mock- and tumor-challenged tadpoles to assess kinetics of Va6 iT cells. Mock challenge was performed by ip injection of APBS without tumor cells. (A, B) Tumor cells were additionally stained with PKH26 Cell Tracer (Sigma) before transplantation to discriminate from CD8<sup>+</sup> T cells. (A) Gating strategy for flow cytometry analysis (top panels), and cytograms showing 3 days following tumor transplantation in PKH26 gate (middle panels) and non-PKH26 gate (bottom panels) obtained by pooling five peritoneal lavages from tumor-transplanted tadpoles. (B) Number of XNC10-T<sup>+</sup> cells in non-PKH26 gate. (C–F) Relative transcript levels of Va6-Ja1.43 iTCR after ff-2 tumor challenge was quantified in peritoneal cavity (C), spleen (D), thymus (E) and liver (F). Each dot represents one tadpole. Dotted black line indicates the limit of qPCR detection. Gene expression was normalized against GAPDH transcript expression and represented as fold change compared with the lowest level of expression. Results are pooled from three independent experiments and presented as the mean  $\pm$  SEM ( $n = 5-17$ ). One-way ANOVA, followed by *post hoc* Tukey's multiple comparisons tests were used to determine the significance of differences among groups and defined as \* $P < 0.05$ , \*\* $P < 0.005$ , \*\*\* $P < 0.0005$ . ns, no statistical significance.

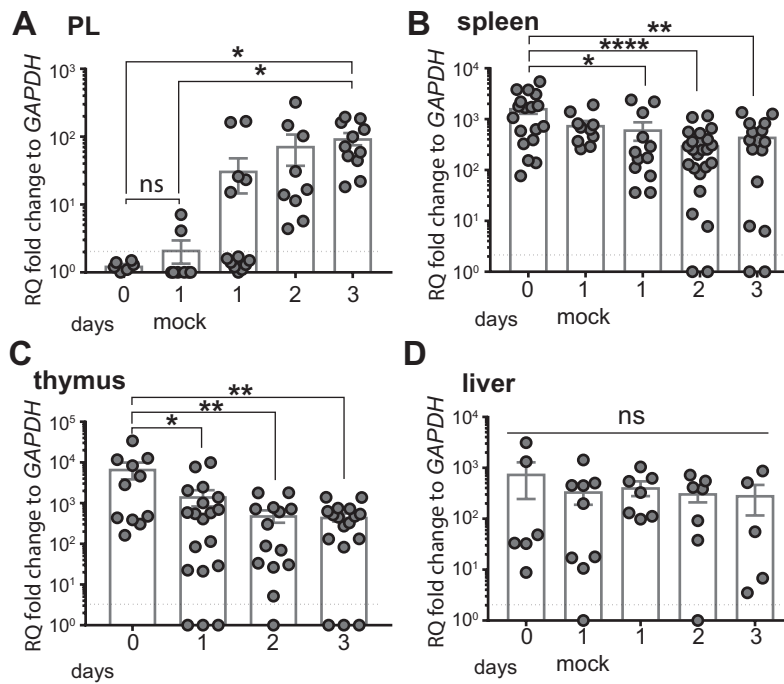


**Figure 2.** Changes in *Va22-Ja1.32* iTCR transcripts following ff-2 tumor transplantation. Tadpoles at the developmental stage 54–55 were ip challenged with  $1 \times 10^5$  ff-2 tumor cells. Peritoneal cells, spleen, thymus and liver were collected from un-, mock- and tumor-challenged tadpoles. Mock challenge was performed by injecting ip APBS only. (A–D) Relative transcript level of *Va22-Ja1.32* iTCR was measured in peritoneal cavity (A), spleen (B), thymus (C) and liver (D) following ff-2 tumor challenge. Gene expression was normalized against *GAPDH* expression and represented as fold change compared with the lowest expression level. Dotted black line indicates qPCR detection limit. Results are pooled from three independent experiments and presented as the mean  $\pm$  SEM ( $n = 6-21$ ). One-way ANOVA followed by *post hoc* Tukey's multiple comparisons tests were used to determine the significance of differences among groups and defined as \* $P < 0.05$ , \*\* $P < 0.005$ , \*\*\*\* $P < 0.00005$ . ns, no statistical significance.

(14,20). We observed a significant decrease in the frequency and cell number of ff-2 tumors in the XNC10 KD Tg tadpoles compared with WT controls, 7 days post-transplantation (Figure 3B). In addition, the forward and scatter profiles of peritoneal cells revealed the accumulation of leukocytes with a distinct size and complexity in the XNC10 KD Tg hosts (Figure 3A, top panel). Intriguingly, the majority of these infiltrating cells were MHC class II<sup>+</sup>. Indeed, although similar in frequency, the numbers of MHC class II<sup>+</sup> peritoneal leukocytes detected were lower in tumor-transplanted XNC10 KD compared with WT recipients (Figure 3C). In contrast, a large fraction (90%) of double-negative (class II<sup>-</sup>/CTX<sup>-</sup>) cells were detected in tumor-transplanted XNC10 KD (Figure 3A bottom panel).

Because the RNAi-mediated XNC10-deficiency is global and established from early embryogenesis, immune mechanisms independent of Va6 iT cells may affect ff-2 tumor tolerance. To address this possibility, we examined the fate of ff-2 tumor within the first 3 days post-tumor challenge. Strikingly, we observed a marked decrease in the frequency of ff-2 tumors to non-tumor cells at day 3 post-tumor challenge in the XNC10 KD Tg hosts (Figure 3D). Concomitantly, the signature transcript levels of neutrophils—granulocyte colony-stimulating factor receptor (GSCF-R) markedly increased at day 3 in XNC10 KD Tg compared with WT hosts (Figure 3E), whereas there was no difference between transcript levels of macrophage colony-stimulating factor receptor between the groups (Supplementary Figure S4, available at *Carcinogenesis* Online). These data suggest that the early tolerance of ff-2 tumors is compromised in the XNC10-deficient tadpoles and that the tumor rejection may involve additional immune effector cells depending on the interactions with XNC10.

### XNC10-T-mediated impairment of Va6 iT cells at the tumor site

Using XNC10 KD Tg tadpoles, we could not exclude the possibility that XNC10 is required for the differentiation and function of immune cells other than Va6 iT cells. Besides the identification of antigen-specific T cells, polymers of MHC molecules, tetramers, can be used to selectively deplete T cells *in vivo* (23). Thus, we tried to deplete or inactivate Va6 T cells using XNC10-tetramers (XNC10-T). During the initial characterization, we noted that XNC10-T induced Va6 iT cell death, especially if not titrated or stained for >30 min. To confirm these observations, we incubated freshly isolated splenocytes for 30 and 90 min on ice with 4 different concentrations of APC-conjugated XNC10-T (5.0, 7.5, 10.0, 12.5  $\mu\text{g}/12.5 \mu\text{l}$ ) (Figure 4A) and determined cell death by propidium iodide staining. After 30 min, minimal Va6 iT cell death was detected at all range of XNC10-T concentrations (Figure 4A, Supplementary Figure S5B, available at *Carcinogenesis* Online). However, Va6 iT cell death markedly increased when the XNC10-T incubation was prolonged to 90 min (Figure 4A, Supplementary Figure S5A, available at *Carcinogenesis* Online). Importantly, XNC10-T only affected the viability of Va6 iT cells because no significant death was measured in the XNC10-T<sup>-</sup> cells (Supplementary Figure S5B, available at *Carcinogenesis* Online). Interestingly, conducting this experiment at room temperature increased XNC10-T induced Va6 iT cell death compared with incubation on ice (Supplementary Figure S5C, available at *Carcinogenesis* Online). **To obtain** *in vivo* evidence, we injected 1  $\mu\text{g}$  of XNC10-T in 10  $\mu\text{l}$  APBS per tadpole ip 1 day before and 1 day after ff-2 tumor transplantation. The tadpoles were sacrificed 9 and 14 days after ff-2 tumor transplantation to allow recovery. We assessed the effects of XNC10-T *in vivo* treatment by determining the expression changes of *Va6-Ja1.43* iTCR



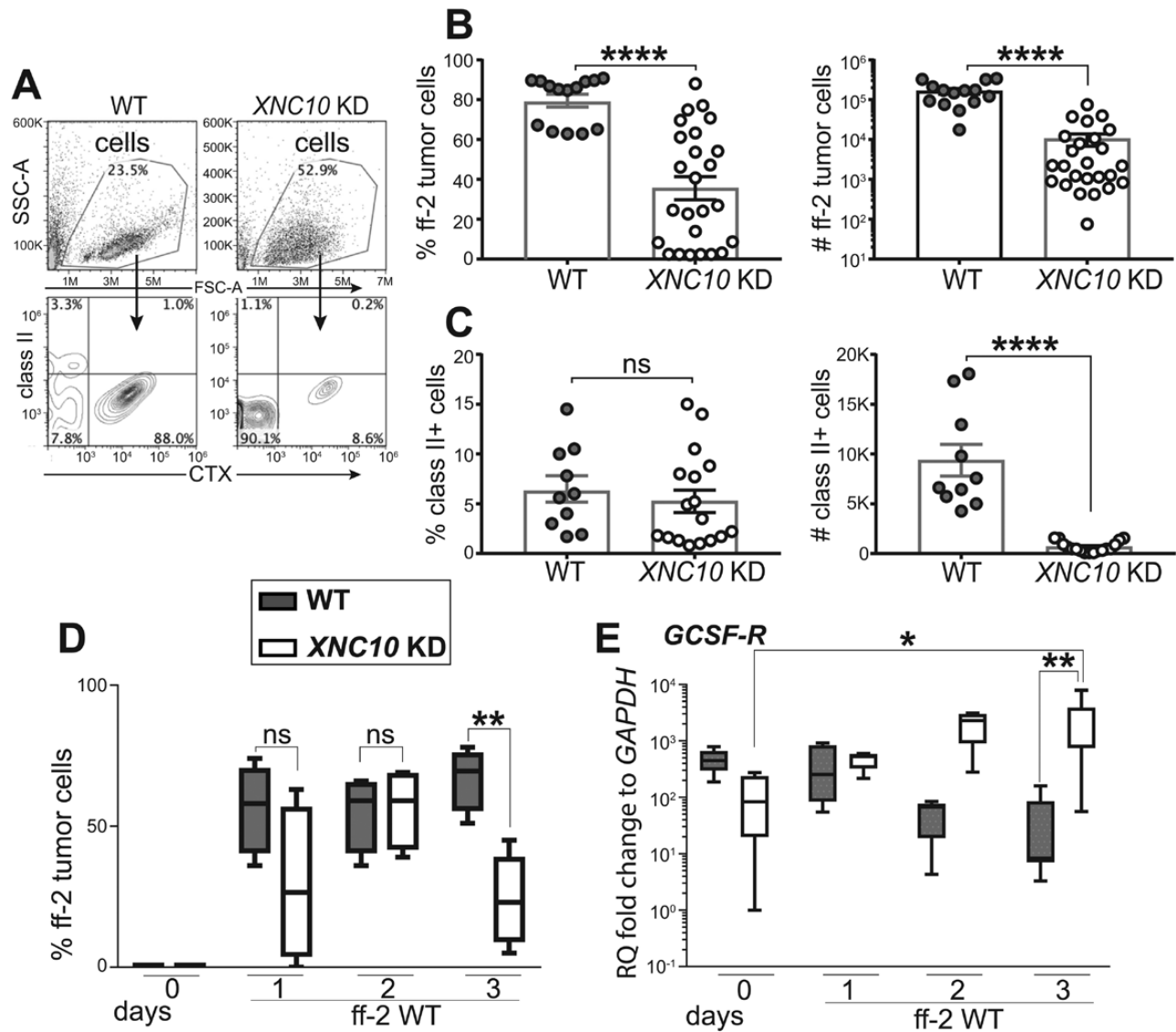


**Figure 3.** Outcome of ff-2 tumor transplantations into XNC10-deficient tadpoles. WT or XNC10 KD Tg F tadpoles at developmental stage 54–55 were ip transplanted with  $1 \times 10^6$  ff-2 tumor cells. At indicated day after transplantation, peritoneal lavages were performed, and cells were subjected to flow cytometry. Frequency and cell number of ff-2 tumor cells were assessed with CTX staining. (A–C) Flow cytometry analysis at day 7 following tumor transplantation. (A) Representative FSC-A/SSC-A plots showing cells tumor and peritoneal cells (top) and CTX/MHC class II staining (bottom) obtained from WT and XNC10 KD Tg tadpoles. (B) Frequencies and numbers of CTX<sup>+</sup> ff-2 tumor cells. (C) Frequencies and numbers of CTX<sup>+</sup>/MHC class II<sup>+</sup> cells. (D) Frequency of retrieved ff-2 tumor cells, stained with CTX, following 3 days after transplantation in WT and XNC10 KD Tg tadpoles. (E) Relative abundance of GCSF-R transcripts at days 1, 2 and 3 after transplantation in WT and XNC10 KD Tg tadpoles. Gene expression was normalized against GAPDH expression and presented as fold change compared with the lowest level of expression. Results were pooled from three independent experiments and presented as the mean  $\pm$  SEM ( $n = 10$ –25). Two-tailed unpaired t test was used to determine significance of differences between groups and defined as \* $P < 0.05$ , \*\* $P < 0.005$ , \*\*\*\* $P < 0.00005$ . ns, no statistical significance.

and of cytotoxic factors associated with iT cells (*perforin*, *FasL*) and by determining tumor growth. The ff-2 tumor-induced increase of *Va6-Ja1.43* iTCR in the peritoneum was significantly ablated at day 9 after the XNC10-T regimen, whereas there were no differences between the experimental groups at day 14 (Figure 4B). In addition, the decrease of *Va6-Ja1.43* iTCR transcripts in the spleen, detected after ff-2 transplantation, was prevented by the XNC10-T treatment (Figure 4B). Interestingly, the XNC10-T treatment significantly increased *Va22-Ja1.32* iTCR at day 9 in the peritoneum (Supplementary Figure S6, available at Carcinogenesis Online). The XNC10-T-induced decrease of *Va6-Ja1.43* iTCR transcripts was accompanied by a significant reduction of *perforin* and *FasL* transcript levels in the peritoneal cavity (Figure 4C). Of note, we also measured the transcripts of *iNOS* and *Arg1*, which reflect the

polarization state of proinflammatory M1 and anti-inflammatory M2 macrophages, respectively. Although the *Arg1* expression was unchanged among experimental groups, *iNOS* transcripts significantly decreased after the XNC10-T-treated tadpoles (Figure 4D). Remarkably, the XNC10-T treatment significantly enhanced ff-2 tumor growth, as indicated by the increased numbers of tumor cells recovered (Figure 4E). In summary, these data suggest that *Va6* iT cells are antitumor effectors that can limit ff-2 tumor growth.

#### Generation of XNC10 KO ff-2 tumor clones via the CRISPR/Cas9 system

We previously showed that 15/0 lymphoid tumors with stable XNC10 KD were acutely rejected by syngeneic LG-15 tadpoles

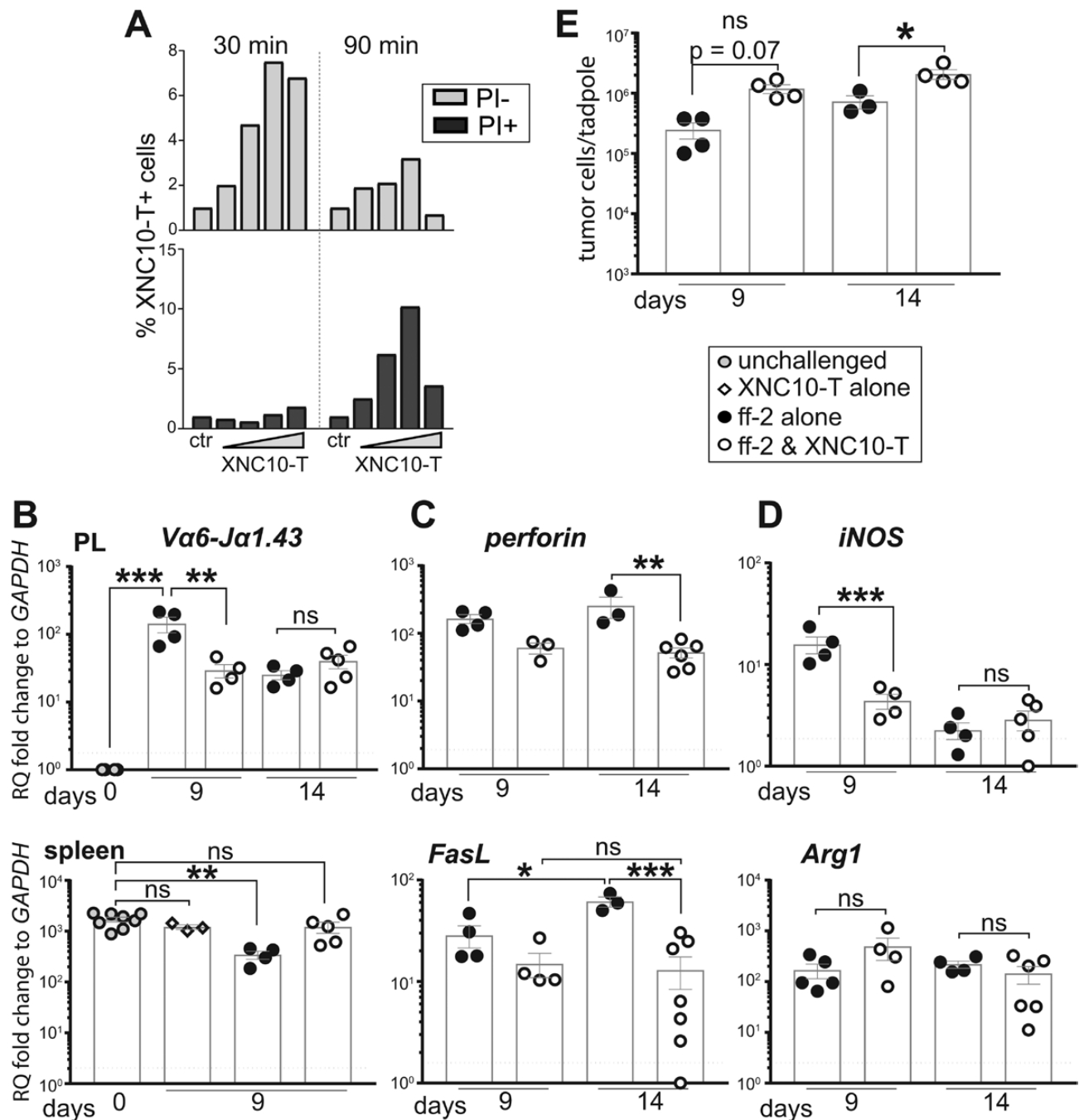


**Figure 4.** XNC10-T impairs Va6 iT cells and promotes ff-2 tumor growth in vivo. (A) XNC10-T induced Va6 iT cell death *ex vivo*. Freshly isolated splenocytes from an adult outbred *X. laevis* were stained with four different concentrations of APC-conjugated XNC10-T (5.0, 7.5, 10.0 and 12.5  $\mu\text{g}/12.5 \mu\text{l}$ ) for 30 and 90 min. Live/dead cell viability dye—propidium iodide (PI) was used to stain dead cells. (B–F) Two doses of 1  $\mu\text{g}$  XNC10-T in 10  $\mu\text{l}$  APBS were ip administered, 1 day before and 1 day after ip ff-2 WT tumor challenge. Peritoneal cells and spleens were collected to assess gene expression by qPCR and tumor cell count (cytospin followed by Giemsa staining). (B) Transcript levels of *Va6-Ja1.43* iTCR were assessed in peritoneal cavity and spleen following XNC10-T administration in ff-2 tumor-bearing tadpoles. (C, D) Transcript levels of *perforin* and *FasL* (C) as well as *iNOS* and *Arg1* (D) were detected in peritoneal cavity. (E) ff-2 tumor cells collected by peritoneal lavage and cell numbers were assessed by cytospin and Giemsa stain. Each dot represents one tadpole. Dotted black line indicates qPCR detection limit. Gene expression was normalized against GAPDH expression and represented as fold change compared with the lowest level of expression. One-way ANOVA followed by post hoc Tukey's multiple comparisons tests were used to determine significance of differences among groups and defined as \* $P < 0.05$ , \*\* $P < 0.005$ , \*\*\* $P < 0.0005$ , ns, no statistical significance.

(14). To investigate whether XNC10 is also critical for ff-2 tumor-induced immune suppression, we generated XNC10 knockout (KO) ff-2 tumor cells via the CRISPR/Cas9 system and homology-directed repair (HDR). After co-transfection of ff-2 tumor cells with two vectors (sgRNA-XNC10-Cas9-mCherry and XNC10-homo-trFP-puro), we selected the clones that incorporated

the HDR-artificial template with puromycin. The fluorescent markers enabled tracking the transfectants by flow cytometry. Within 72 h post-transfection, we detected a population of trFP+ cells that expanded from 6.6 to 64.0% over the following 3 weeks (Figure 5A). Fluorescent microscopy confirmed that an average of 65% ff-2 transfectants were trFP+ (Figure 5A). Using primers

flanking the homologous HRD-template and in the tRFP-puro cassette, we confirmed the correct integration of the tRFP-puro cassette in the XNC10  $\alpha 2$  domain for a subset of transfectants (Figure 5B).

Several XNC10 KO ff-2 clones were obtained by serial dilution and screened at the genome, transcript and cell surface protein levels. The integration of the tRFP-puromycin cassette in the XNC10 gene region should prevent amplification of the XNC10  $\alpha 2$  domain (amplicon of 320 bp), and, thus, indicate the XNC10 gene disruption (Figure 5C). Among the tested clones, #5 and #6 were homozygous XNC10 gene KO (XNC10<sup>-/-</sup>) as genomic primers did not amplify any product. In addition, the XNC10 transcripts were undetectable in these clones, while the expression of several other XNC genes, including XNC1, XNC4 and XNC11, was not altered (Figure 5D). The clone #9 was a heterozygous XNC10 KO (XNC10<sup>+/-</sup>) since only about half of the amount of genomic and transcript products were amplified compared with WT ff-2. This corresponded to ~50% reduction of XNC10 transcript levels consistent with the disruption of one XNC10 allele. The clone #3 did not show any evidence of XNC10 gene disruption or altered gene expression (XNC10<sup>+/+</sup>) despite puromycin resistance. This suggests that the tRFP-puro cassette may have been accidentally integrated elsewhere in the genome. Of note, clone #8 had a mutation in the XNC10 gene that did not involve the

incorporation of the tRFP-puromycin cassette. Importantly, the expression of other highly expressed XNC genes (XNC4, XNC1, XNC11) was unaffected in the all screened clones.

In addition, we used an anti-XNC10 pAb that preferentially binds to XNC10, although it cross-reacts with other XNC molecules (14). The binding of anti-XNC10 pAb correlated with the transcript levels (Figure 5E). Compared with ff-2 WT, the staining intensity of XNC10<sup>-/-</sup> KO ff-2, clone #5, was decreased (median fluorescence intensity: 57 440 versus 10 000). The XNC10<sup>-/-</sup> KO, clone #9, exhibited a smaller decrease in the surface staining (Figure 5E). Of note, XNC10<sup>+/-</sup> KO ff-2, clone #3, also had a slight decrease in anti-XNC10 pAb staining, compared with ff-2 WT. In summary, we utilized the CRISPR/Cas9 system and HDR to specifically knockout the XNC10 gene in ff-2 tumor cells.

### In vitro and in vivo growth of XNC10 KO ff-2 tumor cells

Before transplanting the different XNC10 KO ff-2 clones, we assessed their proliferation in vitro over a period of 72 h (Figure 6A). Trypan blue exclusion staining was used to assess the percentage of dead cells. The proliferation rate of our clones did not significantly deviate compared to WT ff-2 (Figure 6A). As such, XNC10 KO ff-2 clones did not have any detectable in vitro proliferative defects.

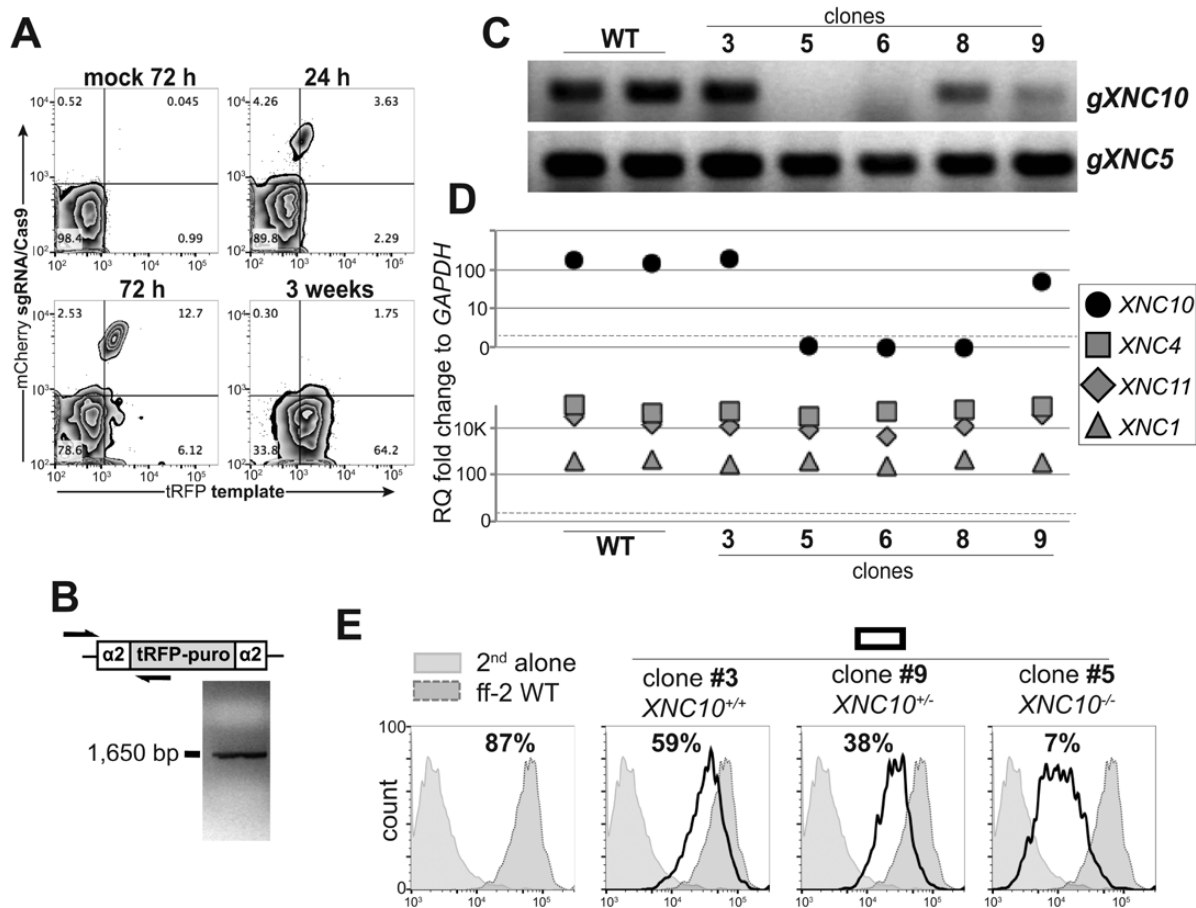


**Figure 5.** Generation and validation of ff-2 XNC10 KO tumor cells. ff-2 cells were transfected via 4D-Nucleofector™ system (Lonza) with two plasmids: sgRNA-XNC10-mCherry-Cas9 and homology template of XNC10  $\alpha 2$  with tRFP-puro cassette. Puromycin-containing media facilitated selection. (A) Transfection efficiency monitored with flow cytometry. (B) Integration of artificial cassette in XNC10  $\alpha 2$  domain, detected by conventional PCR. (C–E) Single cell clones, generated by serial dilution, were screened for the absence of genomic XNC10 PCR product (C), relative expression of XNC10 and other XNC genes (D) and cell surface expression of XNC10, detected by polyclonal  $\alpha$ -XNC10 Ab (E). Gene expression was normalized against GAPDH and represented as fold change compared with the lowest level of expression. MFI, median fluorescence intensity: ff-2 WT—61,315; XNC10<sup>+/+</sup> clone #3—45,048; XNC10<sup>-/-</sup> KO clone #9—38,943; XNC10<sup>-/-</sup> KO clone #5—38,358.

We then measured the growth of XNC10 KO ff-2 clones 7 days after ip transplantation into WT inbred F tadpoles by flow cytometry. The transplanted ff-2 WT, XNC10<sup>+/+</sup> clone #3 and XNC10<sup>+/-</sup> clone #9 had similar tumor cell frequency (Figure 6B). In contrast, the frequency and cell number of the homozygous XNC10<sup>-/-</sup> clone #5 were significantly impaired (Figure 6B and C). Interestingly, the number of CTX<sup>+</sup> tumor cells was also significantly decreased when tadpoles were transplanted with the putative heterozygous XNC10<sup>+/-</sup> clone #9 (Figure 6B and C). In conclusion, these data provide further evidence that functional XNC10 molecules expressed at a sufficiently high level by ff-2 tumor are required to overcome rejection in the tadpoles.

**Discussion**

Due to their immunoregulatory potentials, iNKT cells represent a therapeutic prospect against human cancers (24). However, the

mechanisms that lead to the activation of iNKT cells are only partially known. The analysis of evolutionary conservation of NKT cell functions may aid in a better understanding of NKT cell roles in the context of tumors. The *X.laevis* tadpole is valuable in addressing the evolutionary relevance of NKT cells (25). Apart from being the only ectothermic vertebrate with transplantable lymphoid tumor cell lines and compatible MHC inbred animals, *X.laevis* has well-characterized NKT cell analogs—iT cells interacting with XNC (15,16,18). Here, we identified two iT cell subsets, defined by V $\alpha$ 6 and V $\alpha$ 22 iTCR, probably involved in tumor immune responses, and showed that V $\alpha$ 6 iT cells are antitumoral. We also provide evidence that the ff-2 tumor-induced tolerance can be breached at both the organism and tumor cell levels by targeting the same gene, XNC10.

Our data indicate a rapid infiltration of iT cells to the tumor site consistent with mammalian NKT cell features (7). Although we cannot exclude a possible V $\alpha$ 6 iT cell expansion

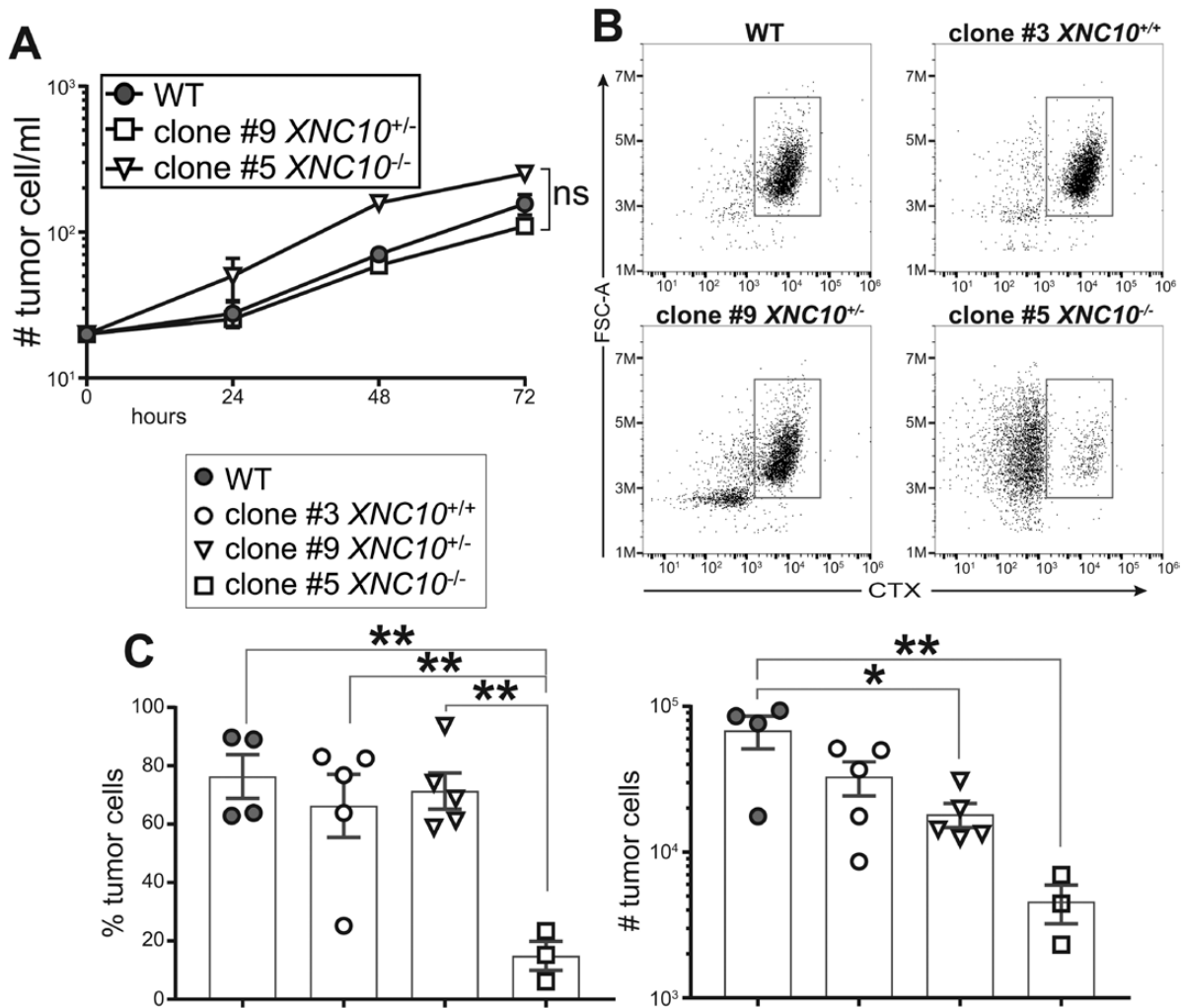


**Figure 6.** XNC10 KO ff-2 tumor cells have no proliferative in vitro defect but are rejected by syngeneic F tadpoles. (A) In vitro proliferation rate of XNC10 KO ff-2 tumor cells, assessed by plating 500 000 cells per well of each tumor clone in triplicates. Cell number was evaluated at 24, 48 and 72 h using a hemocytometer and Trepan blue exclusion staining; percentage of dead cells never reached 5% per well. Values are presented as the mean  $\pm$  SEM. Statistical differences were determined using a nonparametric Mann–Whitney U test. (B and C) Rejection of XNC10 KO ff-2 tumor clones by syngeneic F tadpoles. F tadpoles at the developmental stage 54/55 were ip transplanted with  $1 \times 10^5$  ff-2 tumor cells: WT, non-mutated XNC10<sup>+/+</sup> clone #3, heterozygous XNC10<sup>+/-</sup> KO clone #9, homozygous XNC10<sup>-/-</sup> KO clone #5. At day 7 after tumor transplantation, peritoneal lavages were performed, cells counted and stained with CTX for flow cytometry. (B) Representative flow plots of peritoneal exudates stained with CTX mAb. (C) Frequency and cell number of CTX<sup>+</sup> ff-2 tumor cells. Data pooled from two independent experiments and represented with the mean  $\pm$  SEM ( $n = 3-5$ ). One-way ANOVA followed by post hoc Tukey’s multiple comparisons tests were used to determine the significance of differences among groups and defined as \* $P < 0.01$ , \*\* $P < 0.005$ . ns, no statistical significance among any paired groups.



or a preferential retention in the peritoneum, the recruitment of these cells appears to be a reasonable explanation. It is consistent with the increase of *Vα6* iT cells and their iTTCR transcripts in the peritoneum, concomitant with the decrease of these transcripts in the spleen and thymus. We propose that *Vα6* iT cells are antitumoral because XNC10-T-mediated *Vα6* iT cell depletion results in an increase in tumor cells. Future investigations will establish whether *Vα6* iT cells exert antitumor functions directly or indirectly via other immune cells. Based on previous reports, *Vα6* iT cells are characterized as CD4<sup>+</sup>, CD8α/α<sup>-</sup> or dim, which is also reminiscent of mammalian iNKT cells (14,15). As mammalian CD8/CD4 double-negative liver-derived but not thymic-derived iNKT cells are antitumoral (26), it will also be interesting to investigate whether *Vα6* iT cells derived from different tissues have distinct antitumor potentials.

The *Vα22* iT cell subset is still not well understood. Interestingly, *Vα22* iTTCR transcript levels do not change after virus or microbial infections (16,18). Therefore, the increase of *Vα22* iTTCR after tumor challenge and in the XNC10-T treatment experiment suggests that *Vα22* iT cells are specialized toward tumors. We also found that the distribution of *Vα22* iTTCR transcripts differs between inbred F and outbred animals that were used in the above-mentioned pathogen studies (19). However, this finding is not unique to *Xenopus* as different mouse strains have characteristic iNKT cell tissue allocations (27). Still, the distribution of *Vα22* iTTCR transcripts differs from *Vα6* iTTCR arguing for the relevance of this iT subset in tumor responses. It is probable that one of the XNC molecules interacts with *Vα22* iT cells. For now, we can only speculate about the functions of these two *X.laevis* iT cell subsets in response to ff-2 tumor. The mammalian tumor immunity is directed by the simultaneous activities of antitumor iNKT and protumor type II NKT cells (28). The balance between the activation states of these NKT cell subsets can either promote tumor growth or facilitate tumor eradication. It is plausible that the *Xenopus* immune system has evolved a similar or convergent mechanism based on two antagonistic iT cell subsets.

In addition to the importance of iT cells in tumor immunity, our study shows that tumor tolerance can be controlled by the degree of XNC10 expression on ff-2 tumors. Using the CRISPR/Cas9 system combined with HDR, we generated XNC10 KO ff-2 tumors that were rejected by F tadpoles following transplantation. These findings are in agreement with our previous report in which XNC10 silencing in 15/0 tumor cells rendered those tumors vulnerable to the immune-mediated killing (14). Although both 15/0 and ff-2 tumor cell lines are derived from thymic lymphoid tumors, they are genetically unrelated. Where 15/0 originated from a cloned female frog LG-15 with MHC a/c, ff-2 tumor arose in an inbred F frog MHC homozygous f/f (21). Moreover, unlike 15/0, ff-2 tumors express classical MHC class Ia at low level and have a chromosomal translocation (20,29). Rejection of two different tumors resulting from the XNC10 deficiency suggests that the XNC10 expression by these tumors prevents or overcomes the antitumor immune response. It is noteworthy that ff-2 tumor with a heterozygous XNC10 deletion was also rejected with a slower kinetics. It is possible that a high expression level of XNC10 by tumors overstimulates *Vα6* iT cells and in turn favors a protumor microenvironment.

We have previously proposed that XNC10 and *Vα6* iT cells in *Xenopus* are functional analogs of mammalian CD1d and NKT cells (15). As NKT cells hold a promise against human cancers, the role of CD1d in tumor immunity is under active investigation. The majority of mouse studies have demonstrated that CD1d expression on tumor cells facilitates iNKT cell-mediated tumor eradication and that CD1d-deficient tumors are resistant

to cell-mediated cytotoxicity (9). These reports can be difficult to reconcile with the data presented here. However, some human data are inconsistent with murine models. For example, CD1d expression on leukemia and renal cancers is associated with worse patient survival (30,31). Furthermore, a recent report using human leukemic cells demonstrated that higher CD1d expression correlated with cancer aggressiveness (32). The different outcomes of the CD1d expression on tumor growth may relate to tumor types, stages or CD1d ligands. Different glycolipids binding CD1d elicit opposing protumor or antitumor responses (24,33).

Besides CD1d, human CD1b and CD1c expressed on mouse tumor cell lines promote antitumor responses (34,35). Akin to our results, certain nonclassical MHC class Ib molecules are strongly associated with protumor responses. For example, human leukocyte antigen (HLA)-E and HLA-G are indicators of tumor escape and used as prognostic markers for worsening diseases (36,37). It is thought that the balance between antitumor and protumor activities of different MHC molecules determines tumor tolerance or rejection. Apart from the XNC10 gene, 15/0 and ff-2 tumor cells express other XNC genes, including XNC1, XNC4 and XNC11. It is possible that each of these genes influences tumor fate differently. That notion is supported by our earlier study where 15/0 tumors, deficient in all XNC genes, were more aggressive upon *in vivo* transplantation compared with WT 15/0 tumors (38).

Interestingly, our findings demonstrate that different immune responses can be obtained when XNC10 is impaired at the tumor cell or organism levels. In contrast to WT controls, transgenic XNC10 KD inbred F tadpoles did not support ff-2 tumor growth. Consistent with our results, two reports demonstrated that CD1d<sup>-/-</sup> KO mouse are more resistant to certain types of cancers (39,40). However, these studies did not elucidate a possible mechanism. Here, we observed that the early rejection of ff-2 tumor in the transgenic XNC10 KD hosts was correlated with an increased transcript level of GCSF-R, a signature of neutrophils. It remains to be determined whether silencing of XNC10 affects the development and function of other immune cells such as neutrophils.

It is also possible that distinct ligands presented in the context of XNC10 result in different physiological outcomes. The identity of XNC10 ligand(s) is currently unknown. However, nucleotide sequence comparisons of the putative ligand binding regions have revealed that XNC10 lacks residues that enable peptide binding, suggesting lipid ligands (12,13). Although CD1d performs immune functions via stimulation of iTTCR, other MHC class I-like molecules can ligate with non-TCR receptors. For example, besides presentation of microbial antigens to TCR, H2M3 is recognized by the inhibitory NK receptor Ly49A (reviewed in ref. (41)). Similarly, human HLA-E can interact with TCR expressed on CD8 T cells in responses against *M. tuberculosis* but predominantly ligates with the members of NKG2-CD94 NK receptors (42-44). Notably, HLA-E/Qa-1b ligation to different members of the NKG2-CD94 family results in either activating or inhibitory signals. In the context of tumor immunity, another member of the HLA family, HLA-G, is involved in promoting tumor immune evasion via binding to inhibitory receptor Ig-like transcripts 2 and 4 (ILT2, ILT4) expressed on myelomonocytic cells as well as on NK and T cells (37). Although we have shown that T cell sorted with XNC10-T express the invariant *Vα6-Jα1.14* iTTCR rearrangement (15), this does not exclude a possible interaction of XNC10 with non-TCR receptors. The identification of non-TCR cell receptors in *Xenopus* is limited by the high evolutionary plasticity and minimal sequence similarities of these

10.60

10.65

10.70

10.75

10.80

10.85

10.90

10.95

10.100

10.105

10.110

genes (45). Still, putative activating and inhibitory NK-like receptors in *Xenopus* have been identified (46–48). In addition, *X.tropicalis* and *X.laevis* genome harbor 75 members of Fc-like receptors (49). It would be interesting to see whether XNC10 expressed on tumor cells can interact with either of these Fc-like receptors.

To conclude, our studies provide compelling evidence that MHC class I-like molecules and iT cells are critically involved in tumor immunity, not only in mammals but also across jawed vertebrates as exemplified in *X.laevis*. Furthermore, our experiments provide evidence that the XNC10 gene is critical for the immune evasion strategy of *Xenopus* lymphoid tumors.

### Supplementary material

Supplementary data are available at *Carcinogenesis* online.

### Funding

National Cancer Institute (F31CA192664 to M.B.); National Institute of Allergy and Infectious Diseases (R24-AI-059830 to J.R.); the National Science Foundation (IOS-1456213 to J.R.).

### Acknowledgements

We thank Kun Hyoe Rhoo and Connor McGuire for critical discussions of the data and manuscript, Francisco De Jesús Andino, Ryan Hecht, and Timothy Kwan for the technical assistance and Tina Martin for the animal husbandry.

*Conflict of Interest Statement:* None declared.

### References

1. Godfrey, D.I. et al. (2015) The burgeoning family of unconventional T cells. *Nat. Immunol.*, 16, 1114–1123.
2. Reilly, E.C. et al. (2010) Cytokine dependent and independent iNKT cell activation. *Cytokine*, 51, 227–231.
3. Stetson, D.B. et al. (2003) Constitutive cytokine mRNAs mark natural killer (NK) and NKT T cells poised for rapid effector function. *J. Exp. Med.*, 198, 1069–1076.
4. McEwen-Smith, R.M. et al. (2015) The regulatory role of invariant NKT cells in tumor immunity. *Cancer Immunol. Res.*, 3, 425–435.
5. Pellicci, D.G. et al. (2002) A natural killer T (NKT) cell developmental pathway involving a thymus-dependent NK1.1(-)CD4(+) CD1d-dependent precursor stage. *J. Exp. Med.*, 195, 835–844.
6. Rossjohn, J. et al. (2012) Recognition of CD1d-restricted antigens by natural killer T cells. *Nat. Rev. Immunol.*, 12, 845–857.
7. Brennan, P.J. et al. (2013) Invariant natural killer T cells: an innate activation scheme linked to diverse effector functions. *Nat. Rev. Immunol.*, 13, 101–117.
8. Robertson, F.C. et al. (2014) NKT cell networks in the regulation of tumor immunity. *Front. Immunol.*, 5, 543.
9. Nair, S. et al. (2017) Natural killer T cells in cancer immunotherapy. *Front. Immunol.*, 8, 1178.
10. Flajnik, M.F. et al. (1986) Major histocompatibility complex-encoded class I molecules are absent in immunologically competent *Xenopus* before metamorphosis. *J. Immunol.*, 137, 3891–3899.
11. Salter-Cid, L. et al. (1998) Expression of MHC class Ia and class Ib during ontogeny: high expression in epithelia and coregulation of class Ia and *Imp7* genes. *J. Immunol.*, 160, 2853–2861.
12. Goyos, A. et al. (2011) Remarkable conservation of distinct nonclassical MHC class I lineages in divergent amphibian species. *J. Immunol.*, 186, 372–381.
13. Edholm, E.S. et al. (2014) Unusual evolutionary conservation and further species-specific adaptations of a large family of nonclassical MHC class Ib genes across different degrees of genome

- ploidy in the amphibian subfamily Xenopodinae. *Immunogenetics*, 66, 411–426.
14. Haynes-Gilmore, N. et al. (2014) A critical role of non-classical MHC in tumor immune evasion in the amphibian *Xenopus* model. *Carcinogenesis*, 35, 1807–1813.
15. Edholm, E.S. et al. (2013) Nonclassical MHC class I-dependent invariant T cells are evolutionarily conserved and prominent from early development in amphibians. *Proc. Natl Acad. Sci. USA*, 110, 14342–14347.
16. Edholm, E.S. et al. (2015) Nonclassical MHC-restricted invariant Va6 T cells are critical for efficient early innate antiviral immunity in the amphibian *Xenopus laevis*. *J. Immunol.*, 195, 576–586.
17. Edholm, E.I. et al. (2019) Critical role of an MHC class I-like/innate-like T cell immune surveillance system in host defense against ranavirus (Frog Virus 3) infection. *Viruses*, 11, 3.
18. Edholm, E.S. et al. (2018) Distinct MHC class I-like interacting invariant T cell lineage at the forefront of mycobacterial immunity uncovered in *Xenopus*. *Proc. Natl Acad. Sci. USA*, 115, E4023–E4031.
19. Edholm, E.S. et al. (2016) Evolution of innate-like T cells and their selection by MHC class I-like molecules. *Immunogenetics*, 68, 525–536.
20. Robert, J. et al. (1995) Ontogeny of the alloimmune response against a transplanted tumor in *Xenopus laevis*. *Differentiation*, 59, 135–144.
21. Robert, J. et al. (1998) Evolution of immune surveillance and tumor immunity: studies in *Xenopus*. *Immunol. Rev.*, 166, 231–243.
22. Nedelkovska, H. et al. (2013) Effective RNAi-mediated  $\beta$ 2-microglobulin loss of function by transgenesis in *Xenopus laevis*. *Biol. Open*, 2, 335–342.
23. Kappel, B.J. et al. (2006) Remodeling specific immunity by use of MHC tetramers: demonstration in a graft-versus-host disease model. *Blood*, 107, 2045–2051.
24. Godfrey, D.I. et al. (2018) Unconventional T cell targets for cancer immunotherapy. *Immunity*, 48, 453–473.
25. Banach, M. et al. (2017) Tumor immunology viewed from alternative animal models – the *Xenopus* story. *Curr. Pathobiol. Rep.*, 5, 49–56.
26. Crowe, N.Y. et al. (2005) Differential antitumor immunity mediated by NKT cell subsets in vivo. *J. Exp. Med.*, 202, 1279–1288.
27. Berzins, S.P. et al. (2004) Systemic NKT cell deficiency in NOD mice is not detected in peripheral blood: implications for human studies. *Immunol. Cell Biol.*, 82, 247–252.
28. Terabe, M. et al. (2018) Tissue-specific roles of NKT cells in tumor immunity. *Front. Immunol.*, 9, 1838.
29. Goyos, A., et al. (2009) Tumorigenesis and anti-tumor immune responses in *Xenopus*. *Front. Biosci.*, 14, 167–176.
30. Bojarska-Junak, A. et al. (2014) CD1d expression is higher in chronic lymphocytic leukemia patients with unfavorable prognosis. *Leuk. Res.*, 38, 435–442.
31. Chong, T.W. et al. (2015) CD1d expression in renal cell carcinoma is associated with higher relapse rates, poorer cancer-specific and overall survival. *J. Clin. Pathol.*, 68, 200–205.
32. Gorini, F. et al. (2017) Invariant NKT cells contribute to chronic lymphocytic leukemia surveillance and prognosis. *Blood*, 129, 3440–3451.
33. Brutkiewicz, R.R. (2006) CD1d ligands: the good, the bad, and the ugly. *J. Immunol.*, 177, 769–775.
34. Wang, Y. et al. (2018) Unique invariant natural killer T cells promote intestinal polyps by suppressing TH1 immunity and promoting regulatory T cells. *Mucosal Immunol.*, 11, 131–143.
35. Lepore, M. et al. (2014) A novel self-lipid antigen targets human T cells against CD1c(+) leukemias. *J. Exp. Med.*, 211, 1363–1377.
36. de Kruijf, E.M. et al. (2010) HLA-E and HLA-G expression in classical HLA class I-negative tumors is of prognostic value for clinical outcome of early breast cancer patients. *J. Immunol.*, 185, 7452–7459.
37. Lin, A. et al. (2015) Human leukocyte antigen-G (HLA-G) expression in cancers: roles in immune evasion, metastasis and target for therapy. *Mol. Med.*, 21, 782–791.
38. Goyos, A. et al. (2007) Involvement of nonclassical MHC class Ib molecules in heat shock protein-mediated anti-tumor responses. *Eur. J. Immunol.*, 37, 1494–1501.
39. Ostrand-Rosenberg, S. et al. (2002) Resistance to metastatic disease in STAT6-deficient mice requires hemopoietic and nonhemopoietic cells and is IFN-gamma dependent. *J. Immunol.*, 169, 5796–5804.

11.5

11.10

11.15

11.20

11.25

11.30

11.35

11.40

11.45

11.50

11.55

11.60

11.65

AQ5

11.70

11.75

11.80

11.85

11.90

11.95

11.100

11.105

11.110

	40. Terabe, M. et al. (2006) CD1d-restricted natural killer T cells can down-regulate tumor immunosurveillance independent of interleukin-4 receptor-signal transducer and activator of transcription 6 or transforming growth factor-beta. <i>Cancer Res.</i> , 66, 3869–3875.	
12.5	41. He, Y. et al. (2017) NK cell education via nonclassical MHC and non-MHC ligands. <i>Cell. Mol. Immunol.</i> , 14, 321–330.	
	42. Harrieff, M.J. et al. (2017) HLA-E presents glycopeptides from the <i>Mycobacterium tuberculosis</i> protein MPT32 to human CD8+ t cells. <i>Sci. Rep.</i> , 7, 4622.	
12.10	43. Braud, V.M. et al. (1998) HLA-E binds to natural killer cell receptors CD94/NKG2A, B and C. <i>Nature</i> , 391, 795–799.	
	44. Vance, R.E. et al. (1998) Mouse CD94/NKG2A is a natural killer cell receptor for the nonclassical major histocompatibility complex (MHC) class I molecule Qa-1(b). <i>J. Exp. Med.</i> , 188, 1841–1848.	
	45. Ohta, Y. et al. (2015) Coevolution of MHC genes (LMP/TAP/class Ia, NKT-class Ib, Nkp30-B7H6): lessons from cold-blooded vertebrates. <i>Immunol. Rev.</i> , 267, 6–15.	
	46. Yoder, J.A. et al. (2011) The phylogenetic origins of natural killer receptors and recognition: relationships, possibilities, and realities. <i>Immunogenetics</i> , 63, 123–141.	12.60
	47. Ohta, Y. et al. (2006) Ancestral organization of the MHC revealed in the amphibian <i>Xenopus</i> . <i>J. Immunol.</i> , 176, 3674–3685.	
	48. Guselnikov, S.V. et al. (2010) The amphibians <i>Xenopus laevis</i> and <i>Silurana tropicalis</i> possess a family of activating KIR-related Immunoglobulin-like receptors. <i>Dev. Comp. Immunol.</i> , 34, 308–315.	12.65
	49. Guselnikov, S.V. et al. (2008) The <i>Xenopus</i> FcR family demonstrates continually high diversification of paired receptors in vertebrate evolution. <i>BMC Evol. Biol.</i> , 8, 148.	
		12.70
12.15		
		12.75
12.20		
		12.80
12.25		
		12.85
12.30		
		12.90
12.35		
		12.95
12.40		
		12.100
12.45		
		12.105
12.50		
		12.110
12.55		